Available online at www.sciencedirect.com
ScienceDirect
Journal of Solid State Chemistry 180 (2007) 3469–3478
JOURNAL OF SOLID STATE CHEMISTRY
www.elsevier.com/locate/jssc

Influence of the morphology and impurities of $Ni(OH)_2$ on the synthesis of neutral Ni(II)–amino acid complexes

Vicente Rodríguez-González[a], Eric Marceau[a,*], Michel Che[a,b], Claude Pepe[c]

[a]*Laboratoire de Réactivité de Surface (UMR 7609 CNRS), Université Pierre et Marie Curie-Paris 6, 4 Place Jussieu, 75252 Paris Cedex 05, France*
[b]*Institut Universitaire de France, France*
[c]*Laboratoire de Dynamique, Interactions et Réactivité (UMR 7075 CNRS), Université Pierre et Marie Curie-Paris 6, 4 Place Jussieu, 75252 Paris Cedex 05, France*

Received 18 August 2007; received in revised form 14 October 2007; accepted 15 October 2007
Available online 22 October 2007

Abstract

Synthesis of neutral complexes of Ni^{2+} with amino acids has often been reported on a qualitative basis, with a lack of information on the parameters involved in the dissolution of the nickel-containing solid precursor. This paper reports on a systematic study of the reactivity of $Ni(OH)_2$ toward glycine in aqueous solution. The crystallinity and size of hydroxide particles are found to be key parameters in the rapid glycine-promoted dissolution of the hydroxide and synthesis of $[Ni(glycinate)_2(H_2O)_2]$. These parameters derive from the nature of the salt used to prepare the hydroxide. Ni(II) chloride leads to the most reactive solid precursor, because of the presence of defects in the $Ni(OH)_2$ sheets arrangements, assigned to the substitution of Cl^- ions to OH^- ions at the edges of the particles. The reaction between this hydroxide and glycine at 80 °C is quantitative after 7 min and similar rates of dissolution are obtained with other amino acids, alanine or histidine, the reaction with serine being slower. When the hydroxide contains nitrate or carbonate ions, a glycinato complex with composition similar to $[Ni(glycinate)_2(H_2O)_2]$, but with a different crystal structure, is also formed. Spectroscopic results may suggest a structure involving bridging ligands.

Keywords: Nickel hydroxide; Amino acids; Kinetics; Crystal defects; Infrared spectroscopy; Electrospray mass spectrometry

1. Introduction

Metal complexes with amino acids are used as model compounds in the study of the interactions of proteins with metal cations [1] or, in the case of iron glycinates, as food fortificants to cure infantile anaemia [2]. From the coordination chemistry standpoint, adducts between transition metal ions M^{x+} and x equivalents of $NH_2CH(R)COO^-$ constitute one of the rare classes of complexes soluble in water despite their electrical neutrality. Such neutral complexes are expected to interact with oxidic surfaces by hydrogen bonding, which makes an interesting fundamental case of study for the chemistry relevant to the preparation of heterogeneous supported catalysts. Finally, from the materials chemistry standpoint, the decomposition of oxide-supported bis(glycinato) Ni(II) has recently been shown to lead to the unexpected hexagonal close-packed form of metallic nickel [3].

In most complexes, amino acids behave as bidentate ligands through NH_2 and COO^- ends. Soluble nitrate or chloride salts are usually avoided as metal precursors for the synthesis of these complexes, because they lead to acidic solutions in which protonated forms of the amino acid are present in significant quantity. In the case of Ni(II), the source is often solid hydroxide, hydroxycarbonate (HC) or carbonate [4–10], that is, a poorly soluble form of nickel which does not lower the pH when introduced into water. The complex forms upon reaction of the solid with the amino acid, *via* a ligand-promoted dissolution process. Such processes are well documented in geochemistry [11] and they have been observed during the

*Corresponding author. Fax: +33 1 44 27 60 33.
E-mail address: eric.marceau@upmc.fr (E. Marceau).

0022-4596/$ - see front matter © 2007 Elsevier Inc. All rights reserved.
doi:10.1016/j.jssc.2007.10.015

preparation of oxide-supported catalysts, with anions such as molybdates or tungstates extracting cations from the support to form heteropolyanions [12,13].

A survey of the literature on reactions of Ni(II) solid precursors with the most simple amino acid, glycine, nevertheless shows that parameters ruling the dissolution of the solid, and thus the rate of the complex formation (*trans*-diaquabis(glycinato-O,N) Ni(II), [Ni(glycinate)$_2$ $(H_2O)_2$], hereafter referred to as nickel bisglycinate), are not clearly identified. Most authors use the procedure established by Stosick [4], in which an excess of solid is added into a warm solution of glycine. Because part of the nickel precursor, used in excess, is not consumed, the reaction kinetics and completion are difficult to determine precisely. Furthermore, the products resulting from the reaction and crystallization are rarely characterized besides elemental analyses.

The aim of this paper is to identify the parameters ruling the dissolution of $Ni(OH)_2$, a precursor whose structural characteristics can be varied, when contacted with a solution of glycine. The selectivity of the reaction leading to nickel complexes is also studied and linked to the characteristics of the precursor. The fastest route of synthesis identified is then extended to amino acids other than glycine, in order to verify if a series of bis(amino acid) complexes can be prepared by this procedure.

2. Experimental

2.1. Nature of the hydroxides and synthesis of the complexes

Four types of $Ni(OH)_2$ solid precursors were used:

- a commercial hydroxide (Aldrich, 63 Ni wt%), hereafter referred to as H;
- a hydroxide prepared by stoichiometric precipitation of $Ni(NO_3)_2 \cdot 6H_2O$ (Aldrich, purity 99.99%) with KOH (Prolabo), referred to as HN;
- a hydroxide prepared by stoichiometric precipitation of $NiCl_2 \cdot 6H_2O$ (Aldrich, purity 99.99%) with KOH (Prolabo), referred to as HChl and
- a hydroxide prepared by precipitation of $Ni(NO_3)_2 \cdot 6H_2O$ (Aldrich, purity 99.99%) with urea (Prolabo) decomposed at 90 °C, referred to as HT.

HN and HChl were prepared by reaction between 0.43 mol of Ni(II) salt and 0.86 mol KOH in 1 L of aqueous solution. A green precipitate of nickel hydroxide formed and the suspension was left under stirring for 3 h. After decantation and filtration, the gel was dried in static air at 80 °C for 12 h. The solid obtained was then washed with 100 mL of water in order to eliminate KNO_3 or KCl impurities, and then dried a second time at 80 °C for 5 h. HT was synthesized following the method and proportions reported by Burattin et al. [14]. The zero-point charge of the hydroxides was measured by immersion [15] to be close to 8 at room temperature, in agreement with earlier data [16]. It is reported to decrease to 7 at 60 °C [16].

The synthesis of complexes between Ni(II) and amino acids (Aldrich, purities >99%) was carried out with glycine (gly, NH_2CH_2COOH), L-alanine (ala, $NH_2CH(CH_3)COOH$), L-serine (ser, $NH_2CH(CH_2OH)COOH$) and L-histidine (his, $NH_2CH(CH_2C_3H_3N_2)COOH$). In the formula of the complexes, the notations gly, ala, ser and his refer to the basic unprotonated form of the amino acid, i.e., containing the $–CHNH_2(COO^-)$ moiety. The reaction mechanism was studied in the case of glycine only. The reaction was performed by adding solid $Ni(OH)_2$ under stirring to a warm 0.27 mol L^{-1} solution of amino acid (molar ratio amino acid/Ni = 2, T = 60 or 80 °C). $Ni(OH)_2$ was seen to dissolve and the solution to take the colour of the complex formed, blue for gly, ala and ser, purple for his. The dependence of the reaction rate as a function of the hydroxide nature as well as details concerning the complexes separation and crystallization are presented in Section 3.

2.2. Characterization

Elemental analyses were performed at the CNRS Service of Analysis in Vernaison (France). Nickel and chlorine were quantified by ICP; carbon, hydrogen and nitrogen, by catharometry after fast calcination of the sample in air; nitrates by ionic chromatography and carbonates by acidimetric titration after dissolution of the solids in an acid solution.

Powder X-ray diffraction (XRD) measurements were performed at room temperature on a Siemens D500 diffractometer, using radiation Kα of copper (1.5418 Å). XRD was also used to evaluate the size of crystalline domains of $Ni(OH)_2$, applying the Laue–Scherrer equation to single diffraction peaks. Powder patterns were simulated from published crystal structures using the CrystalDiffract code from Crystalmaker Software Ltd. (United Kingdom).

Nitrogen adsorption–desorption isotherms were performed at –196 °C with a Micromeritics ASAP 2010 apparatus, after pretreatment at 150 °C in vacuum. The BET model was used to estimate specific surface areas. Combined differential thermal and thermogravimetric analyses (DT-TGA) were obtained with a Seiko DT-TGA 320 module operated by a Seiko SSC5200 disc station, with a heating rate of 7.5 °C min^{-1} in flowing N_2 (50 mL min^{-1}). For scanning electron microscopy (SEM), dry powders were coated with gold in a Balzers Union SCD 40 sputter-coater and studied on a Cambridge Stereoscan 120 instrument at an accelerating voltage between 15 and 20 kV.

Infrared (IR) spectra recorded on KBr pellets were collected with an FT-IR M-1700 Perkin-Elmer spectrometer with a 4 cm^{-1} resolution. The diffuse reflectance infrared Fourier transform spectra of anhydrous sodium glycinate NH_2CH_2COONa (provided as $NH_2CH_2COONa \cdot xH_2O$, Aldrich) and [Ni(glycinate)$_2(H_2O)_2$] after dehydration were recorded with a 4 cm^{-1} resolution (128 scans) on

a Bruker IFS66 V spectrometer equipped with a mercury cadmium telluride detector. Dehydrations took place at 150 °C in an environmental chamber (Collector, Spectra-tech) under air flow (100 mL min^{-1}) overnight. The sample was dispersed into industrial single-crystalline diamond powder (IR-transparent and diffusing matrix) with an average particle size of 6 μm (10 wt% of the compound in diamond). The final spectrum was obtained by dividing the absorption spectra intensity by the diamond reference absorption spectra intensity recorded in the same thermal conditions, and submitting to the Kubelka–Munk transform. Raman spectra were recorded on powders with a modular HL5R spectrometer equipped with a microscope (Kaiser Optical Systems, Inc.), a near-IR laser diode working at 785 nm, a charge coupled device detector providing fast collection of Raman data from 100 to 3450 cm^{-1} (average resolution 2 cm^{-1}) and holographic Notch filters. UV–visible–near infrared (UV–vis–NIR) spectra of the crystallized complexes were recorded in the reflectance mode with a resolution of 1 nm on a Cary 5 spectrometer (Varian) equipped with an integration sphere, using Teflon as reference.

Mass spectrometry measurements were conducted in positive ion mode using an ion trap mass spectrometer (ESQUIRE, Bruker, Bremen, Germany) equipped with external electrospray ionization (ESI) source (Analytica, Brandford, CT, USA). Ions were formed by electrospraying a solution mixture containing products at 0.0001 M, diluted in a mixture of CH_3OH/H_2O (1:1). The following source voltages were used: capillary −3500 V, end plate −2800 V, capillary exit +45 V and skimmer +10 V. The source temperature was set at 180 °C. The solution was introduced into the ESI source at a flow rate of 2.5 L min^{-1} using a syringe pump. The m/z range was 50–1500 Th ("standard" mode) with a resolution of 1 Th (width at half height). Each peak includes two components, coming from ^{58}Ni and ^{60}Ni, respectively. For this reason, a couple of m/z will be given for each ion mentioned.

3. Results

3.1. Characterization of the hydroxides

X-ray diffractograms (Fig. 1, left) show that the hydroxides are of two types [14,17,18]:

- Hydroxides HChl, HN and H belong to the β-$Ni(OH)_2$ variety, in which parallel $Ni(OH)_2$ sheets are stacked regularly along the vertical axis c of the structure.
- Hydroxide HT belongs to the turbostratic α-$Ni(OH)_2$ variety, in which sheets exhibit some disorder in their vertical arrangement.

In both cases, the first diffraction peak (reflection (001)) leads to the interplanar distance d_{001} between brucite-like $Ni(OH)_2$ sheets (Table 1). The lower position of the line for

Table 1
Structural characteristics of the hydroxides

Hydroxide	Interplanar distance d_{001} (nm)	Size of organized domains along c (nm)	Number of sheets organized along c
HT	0.722	13	18
H	0.461	16	35
HN	0.460	7	15
HChl	0.465	3	6

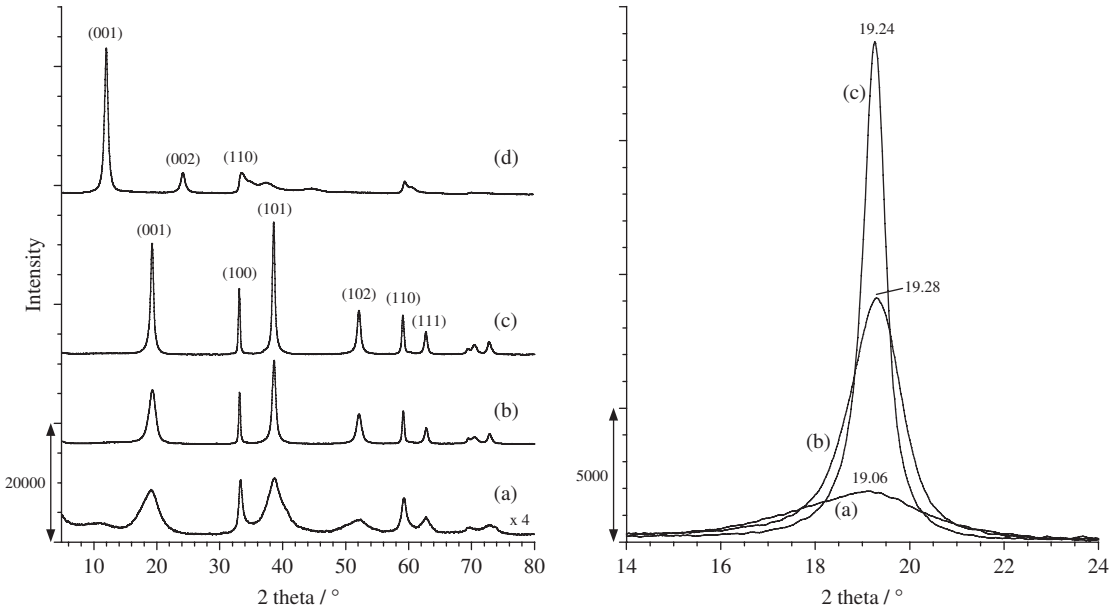

Fig. 1. Left: X-ray diffractograms of hydroxides: (a) HChl; (b) HN; (c) H; (d) HT. Right: zoom on the first diffraction line of hydroxides: (a) HChl; (b) HN; (c) H.

HT, due to a larger interplanar distance in agreement with literature data [14,19], is explained by the intercalation of water or ionic species between the disorganized sheets. A broad peak at $2\theta = 11^\circ$ for HChl may also be due to some intercalated species.

The three samples of β-$Ni(OH)_2$ differ by their crystallinity. For the same amount of hydroxide, the peaks intensity increases along the series HChl < HN < H. Peaks corresponding to reflections within the (a, b)-oriented $Ni(OH)_2$ sheets, for example (100) or (110), are narrow for the three hydroxides, while reflections involving a vertical component (Miller index $l \neq 0$) give broader peaks along the series H < HN < HChl. The Laue–Scherrer analysis of the (100) and (001) peaks shows that crystallized domains along axis a are of similar size (≈ 35 nm), while the organization of sheets along axis c is much diminished for HN and especially HChl (Table 1).

Finally, the (001) peak of HChl shifts toward low angles compared to HN and H (Fig. 1, right), indicating that the mean interplanar distance is larger by 0.03 nm in HChl than for the two others. Moreover, the peak is asymmetric with a broader shoulder at low angles, revealing a distribution of distances along c beyond 0.465 nm due to some structure defects.

The size of organized domains along c and the value of d_{001} allow one to evaluate the average number of sheets organized vertically in the structure of the four hydroxides (Table 1). H appears to be the most organized and HChl the most disorganized. HN and HT differ by their structure, but both exhibit an intermediate degree of organization.

At the micrometric scale (SEM), hydroxide H appears to be an agglomerate of regular spheres of 3 μm in diameter (Fig. 2a), themselves made of rose-like arranged 600 Å-thick platelets (Fig. 2b). In contrast, particles of HChl are disorderly compacted with no regular pattern at any magnification (Fig. 2c and d). Finally, HN (Fig. 2e) and HT (Fig. 2f) are made of a mixture of 10–50 μm well-shaped plates and smaller disorganized entities resembling HChl. Specific surface areas accordingly decrease along the series HChl ($125\,m^2\,g^{-1}$) > HT ($80\,m^2\,g^{-1}$) > HN ($65\,m^2\,g^{-1}$) > H ($30\,m^2\,g^{-1}$).

The composition of the hydroxides was determined by chemical analysis, IR and TGA. The theoretical nickel content (63 wt%) is measured only for hydroxide H (Table 2). Lower contents for the others are explained by the presence of impurities (Cl^- or NO_3^- ions for HChl and HN, respectively), intercalated anions (CO_3^{2-} can be quantified in the case of HT) and water, as evidenced by the low-temperature weight loss detected by TGA. The second weight loss corresponds to the decomposition of $Ni(OH)_2$ into NiO and H_2O (theoretical weight loss expected: 19%), and also of the anions retained on or inside the hydroxide [20], as shown by the large value for HT. Among the four hydroxides, HChl decomposes at the lowest temperature, which can be correlated to its low structural organization.

IR allows one to identify intercalated water (mostly in the case of HT, δ(OH) band at $630\,cm^{-1}$) and the anionic species present in the hydroxides (except chloride ions): isocyanates resulting from the decomposition of urea in HT (bands at 1281, 2182 and $2214\,cm^{-1}$), nitrates in HN, H and HT (bands at 994, 1300, 1382 and $1430–1491\,cm^{-1}$), carbonates in HT, HChl and H (bands at ca. 1065 and $1375\,cm^{-1}$) [14,17,20–24] (Supplementary Material, Fig. S1).

All these data lead to the composition of the four hydroxides (Table 2), assuming that

- as stated in Ref. [14], $Ni(OH)_2$ sheets in turbostatic HT are non-stoichiometric and the positive charges resulting from the missing OH^- ions are compensated by intercalated anions,
- nitrate ions are not intercalated between HN sheets (which would result in a larger interplanar distance [25]) but adsorbed on the hydroxide, because the position of the (001) reflection is identical for HN and H and
- Cl^- ions may be attached to the structure, thus increasing d_{001} of HChl.

Finally, nitrates in HT and carbonates in H and HChl have not been mentioned in the formula because their quantity is too low.

The proportion of water intercalated in HT is difficult to determine exactly (60% assuming that the first weight loss corresponds to adsorbed water only). Water in β-hydroxides is considered mostly as adsorbed; its content increases with the extent of structure disorganization and with the related specific surface area of the hydroxide (H < HN < HChl).

3.2. Reactivity of the hydroxides toward glycine

The initial pH of the gly solution is 6, as expected for a solution containing an amphoteric compound of $pK_a = 2.36$ and 9.56 [11]. The major form is thus zwitterionic, $NH_3^+CH_2COO^-$. Upon reaction with $Ni(OH)_2$, the pH rises to 7, which is explained by the consumption of both gly and $Ni(OH)_2$ and formation of nickel glycinate, which has no acidobasic properties. In this pH range, thermodynamics predicts some dissolution of $Ni(OH)_2$ even in absence of ligands ($K_s = 5.47 \times 10^{-16}$) [26]. A blank experiment performed without gly showed that in our experimental conditions and at that time scale, dissolution of hydroxides is minor (less than 5% solubilized after 5 h at 60 °C). Moreover, there is no reaction between gly and Ni(II) ions issued from nickel nitrate, even at pH raised to 7 by adding a few drops of ammonia solution, despite the chelating character of gly. It can be concluded that the reaction between gly and hydroxide occurs at the solid–liquid interface and that $Ni(OH)_2$ dissolution is mostly promoted by gly. The reaction is faster at 80 than at 60 °C; to improve the precision of

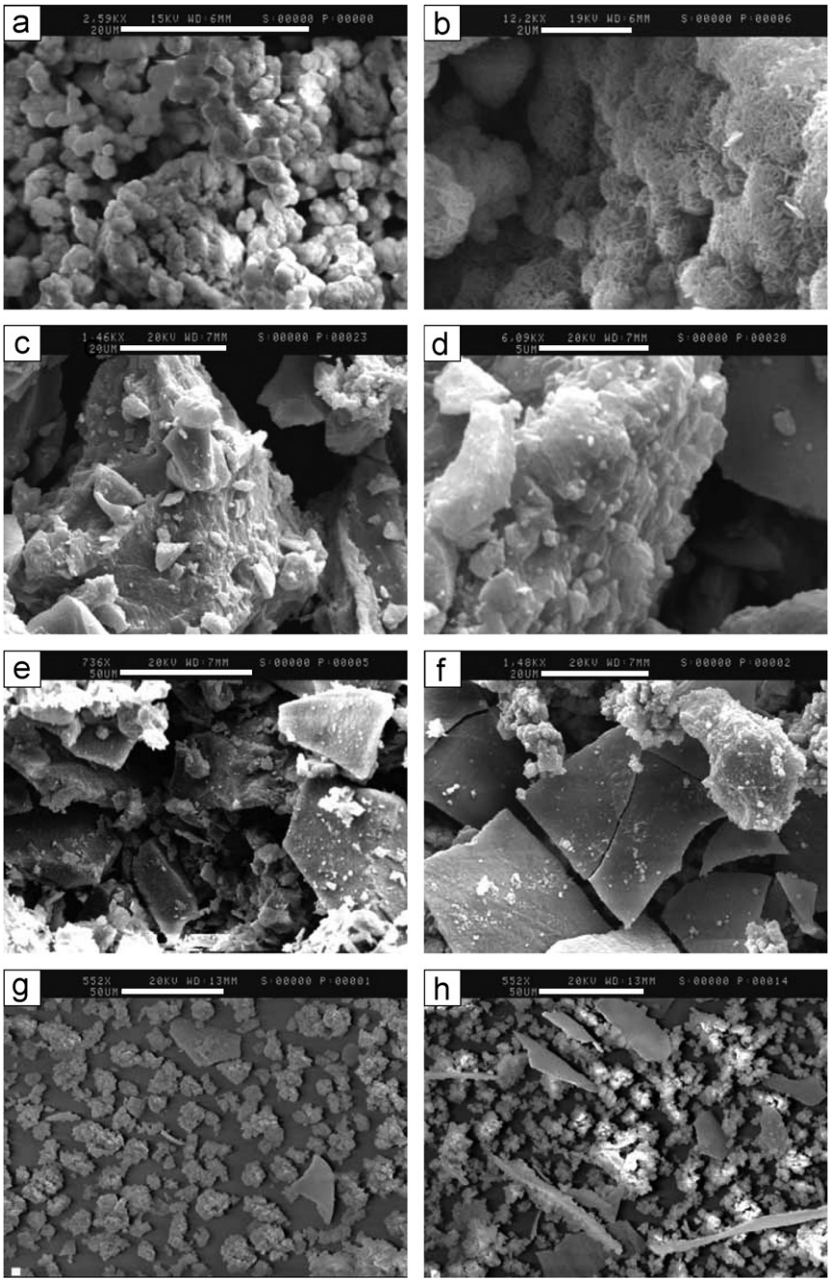

Fig. 2. SEM micrographs of hydroxides: (a, b) H; (c, d), HChl; (e) HN; (f, g) HT; (h) HT after 900 s of reaction with glycine.

Table 2
Composition of the hydroxides, as deduced from chemical analysis and TGA

Hydroxide	Ni (wt%)	N or Cl (wt%)	NO_3^- or CO_3^{2-} (wt%)	T range of first TG event (°C)	First weight loss (%)	T range of second TG event (°C)	Second weight loss (%)	Proposed formula	Estimation of n
HT	49	3.55 (N)	3.60 (CO_3^{2-})	30–270	6	270–350	32	$Ni(OH)_{1.56}(OCN)_{0.31}(CO_3)_{0.07} \cdot nH_2O$	$0.5 \leqslant n \leqslant 1$
H	63	–	–	30–230	2.5	230–430	22	$Ni(OH)_2 \cdot nH_2O$	$0.05 \leqslant n \leqslant 0.1$
HN	58	< 1 (N)	4.15 (NO_3^-)	30–230	2	230–470	22	$Ni(OH)_2.0.06NO_3^- \cdot nH_2O$	$0.1 \leqslant n \leqslant 0.2$
HChl	59	2.00 (Cl)	–	30–205	7.5	205–350	23	$Ni(OH)_{1.95}Cl_{0.05} \cdot nH_2O$	$0.3 \leqslant n \leqslant 0.4$

measurements; the kinetic study was carried out at 60 °C, for which the reaction is slower.

Reactants being used in stoichiometric proportions, the reaction is complete when a clear blue solution of nickel glycinate is obtained, with $Ni(OH)_2$ present only as traces. It takes 30 h (1.08×10^5 s) for H, 3 h (1.08×10^4 s) for HN and HT, and only 15 min (900 s) for HChl. The dissolution kinetics has been studied for H, HT and HChl, by collecting $Ni(OH)_2$ by filtration at various times and weighing it after drying at 100 °C (Fig. 3). Samples were not washed before drying in order to retain any organic molecules adsorbed; it was checked that the weight content of organic matter was below 2% and did not alter mass measurements.

The durations needed to complete the reaction for the different hydroxides differ by one order of magnitude. For H and especially HT, the specific surface area measured at the end of the first steep part of the dissolution curve decreases compared with the initial value, which is not the case for HChl. This coincides with the statistical increase of the proportion of larger plates in the fractions examined by SEM (Fig. 2e and f), thus with the consumption of the smaller particles exhibiting larger specific surface area. In order to check if such difference of reactivity could be explained by the specific surface areas and size of the crystallites alone, average dissolution rates were normalized to 1 m^2 of surface exposed, following Ref. [11] (Table 3). Normalized rates calculated by m^2 still vary with the type of hydroxide, with a reaction on HChl faster by a factor 2.5 compared with HT and 15 compared with H. The key parameter of $Ni(OH)_2$ dissolution is thus not the crystalline variety or the specific surface area, but the presence of more reactive sites.

After 2 min of reaction, the diffractogram of HChl is identical to the initial pattern, indicating the absence of gly intercalation. IR nevertheless shows that the spectrum of the hydroxide after 2 min of reaction differs from that of

Table 3
Evolution of the hydroxides specific surface area during reaction and normalized dissolution rate

Hydroxide	Specific surface area before reaction ($m^2 g^{-1}$)	Time t of reaction (s)	Specific surface area at time t ($m^2 g^{-1}$)	Normalized average dissolution rate ($mmol\, m^{-2} s^{-1}$)
HChl	125	120	135 (+8%)	15×10^{-4}
HT	80	900	50 (−37%)	6×10^{-4}
H	30	900	25 (−16%)	10^{-4}

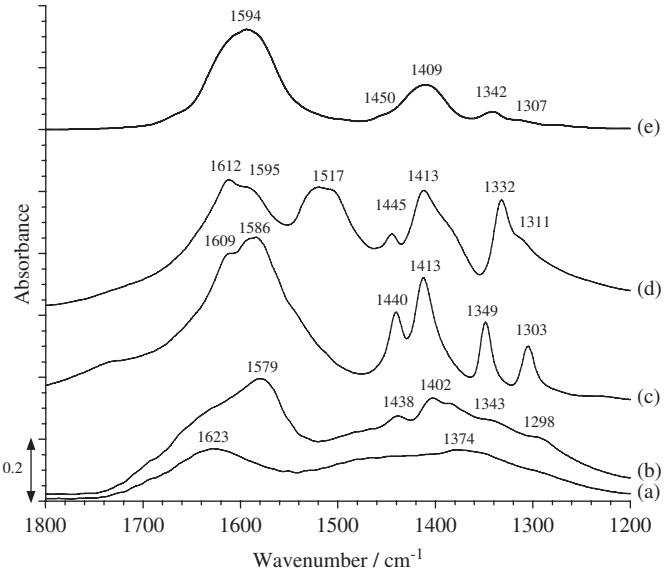

Fig. 4. Infrared spectra recorded at room temperature of (a) hydroxide HChl, (b) hydroxide HChl after 120 s of reaction with glycine, (c) $[Ni(gly)_2(H_2O)_2]$, (d) solid glycine $NH_3^+CH_2COO^-$ and (e) dehydrated sodium glycinate, $NH_2CH_2COO^-Na^+$. Spectra (a)–(d) have been recorded in transmission in KBr, spectrum (e) in diffuse reflectance mode.

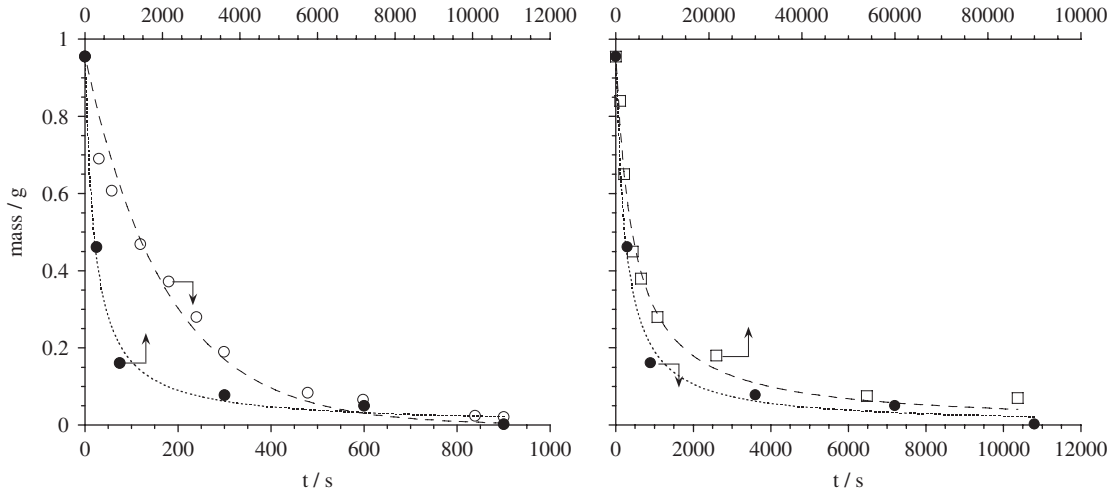

Fig. 3. Evolution of the mass of nickel hydroxide remaining in suspension as a function of time of reaction with glycine. Left: HChl (○) and HT (●). Right: HT (●) and H (□).

the pristine hydroxide, with the presence of bands due to organic molecules (Fig. 4). A comparison with spectra of dehydrated $NH_2CH_2COO^-$ Na^+ and solid glycine $NH_3^+CH_2COO^-$ evidences the absence of the band at 1517 cm^{-1} characteristic of NH_3^+ [27,28]. During reaction, glycine thus adsorbs on $Ni(OH)_2$ as $NH_2CH_2COO^-$, as anticipated from the position of the other bands, close to those of both sodium glycinate and nickel bisglycinate ($\nu_{as}(COO^-)$ at 1579 cm^{-1}, $\delta(CH_2)$ at 1438 cm^{-1}, $\nu_s(COO)$ at 1402 cm^{-1}, $\omega(CH_2)$ at 1343 cm^{-1}, tw(NH_2) at 1298 cm^{-1}) [28,29]. The intermediate state of reaction should thus be very close to the coordination of gly in nickel glycinate, i.e., bidentate ligand coordinated to the hydroxide.

When HChl reacts with amino acids at 80 °C, completion occurs within 7 min for gly, ala and his, and 30 min for ser. $Ni(OH)_2$ which has not reacted (<1%) is eliminated by filtration of the hot solution. After cooling to 5 °C, it is checked by filtration that no nickel hydroxide remains in solution. Crystallization of the complexes takes place in two steps: (i) concentration of the filtrate to half of its volume by Rotavapor evaporation; (ii) addition of an identical volume of commercial ethanol under stirring (30 min), followed by decantation overnight. However, the water–ethanol solution containing Ni(II)–ser complexes has to be left to evaporate to a volume of 5 mL before crystallization occurs, due to the hydrophilicity of the side chain in ser which increases the solubility of the complex. In all cases, yields relative to nickel amount to ca. 60%. Complexes collected by filtration are identified both by elemental analysis (Table 4) and XRD (Fig. 5a and c–e), by comparison with the positions of diffraction lines expected from the crystal structure [8,13,31,32] and calculated using Crystal Diffract software (see Supplementary material, Tables S1–S4, which also contains the UV–visible spectra of the solid complexes [32–35], SFig. 2). $[Ni(ala)_2(H_2O)_2]$ crystals as collected had to be exposed for one night to water vapour in a humidificator so as to reach the degree of hydration associated to the structure published earlier [30]. $[Ni(ser)_2(H_2O)_2]$ crystals also contain water of crystallization, in a proportion which is difficult to ascertain precisely by chemical analyses. The non-centrosymmetric environment of nickel ions in these two complexes leads to a splitting of their absorption bands in the UV–visible spectra; five bands are indeed detected for the serinate complex, at 352, 382, 596, 880 and 1068 nm.

3.3. Influence of the nickel precursor on the selectivity of the reaction

In order to increase the synthesis yield, it was attempted to collect the complexes prepared from gly and HChl not by precipitation in ethanol, but by a quasi-complete

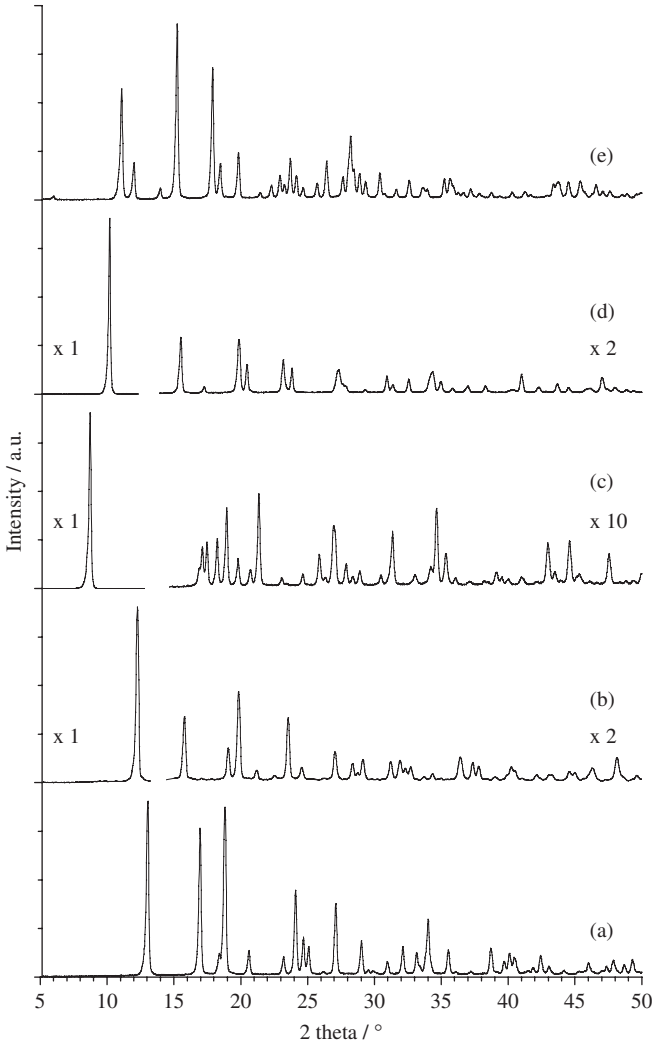

Fig. 5. Experimental X-ray diffractograms of (a) $[Ni(gly)_2(H_2O)_2]$, (b) $[Ni(gly)_2(H_2O)_2]$ (HC), (c) $[Ni(ala)_2(H_2O)_2]\cdot 2\ H_2O$, (d) $[Ni(ser)_2(H_2O)_2]\cdot 0.33\ H_2O$ and (e) $[Ni(his)_2]\cdot H_2O$.

Table 4
Elemental analyses of the Ni(II)–aminoacids complexes

	$[Ni(gly)_2(H_2O)_2]$ $C_4H_{12}N_2O_6Ni$		$[Ni(gly)_2(H_2O)_2]$ (HC) $C_4H_{12}N_2O_6Ni$		$[Ni(ala)_2(H_2O)_2]\cdot 2\ H_2O$ $C_6H_{20}N_2O_8Ni$		$[Ni(ser)_2(H_2O)_2]\cdot 0.33\ H_2O$ $C_6H_{16,66}N_2O_{8,33}Ni$		$[Ni(his)_2]\cdot H_2O$ $C_{12}H_{18}N_6O_5Ni$	
	Found	Calc.	Found	Calc.	Found	Calc.	Found[a]	Calc.	Found	Calc.
Ni (wt%)	23.85	24.2	23.8	24.2	18.85	19.15	18.75	19.0	14.9	15.25
C (wt%)	19.65	19.8	19.9	19.8	23.25	23.45	23.15	23.35	37.3	37.45
H (wt%)	5.0	4.95	5.05	4.95	6.55	6.5	5.5	5.4	4.65	4.7
N (wt%)	11.4	11.55	11.4	11.55	9.15	9.15	8.85	9.0	21.5	21.8

[a]Can also correspond to $[Ni(ser)_2(H_2O)_2]\cdot 0.66\ H_2O$ (Calc. Ni 18.7; C 22.9; H 5.5; N 8.9).

evaporation of water in the Rotavapor. However, XRD showed that the resulting phase is not pure. The same extra peaks were present in larger quantity when HN or HT was the precursor and the procedure of synthesis and crystallization described above was followed. It was found that the contaminating phase, characterized by a set of XRD lines (Fig. 5b, Table 5), could be prepared separately by using Ni(II) hydroxycarbonate $NiCO_3 \cdot 2\ Ni(OH)_2 \cdot 4\ H_2O$ (Fluka, 46 Ni wt%) as precursor. This phase will be noted hereafter $[Ni(gly)_2(H_2O)_2]$ (HC), as opposed to bisglycinate $[Ni(gly)_2(H_2O)_2]$ synthesized from HChl. The two forms cannot be distinguished by elemental analyses (Table 4), UV–visible spectroscopy or thermal analyses. It was possible neither to obtain single crystals, nor to extract unit cell parameters from its powder pattern, whether derived from the monoclinic structure of $[Ni(gly)_2(H_2O)_2]$ or not.

$[Ni(gly)_2(H_2O)_2]$ (HC) was consequently assumed to contain a mixture of phases related to $[Ni(gly)_2(H_2O)_2]$, a hypothesis supported by two observations. First, solid mixtures of $[Ni(gly)_2(H_2O)_2]$ and $[Ni(gly)_2(H_2O)_2]$ (HC) can be totally converted into $[Ni(gly)_2(H_2O)_2]$ (HC) by introduction into ethanol, stirring, filtration and drying at 100 °C. Second, electrospray ionization MS analysis of the two compounds dissolved in a water/methanol mixture reveals strong differences. In the analyser, $[Ni(gly)_2(H_2O)_2]$ mainly provides cations corresponding to the intact complex in hydrated forms: m/z 157/158 ($[Ni(gly)_2(H_2O)_2](H_2O)_4^{2+}$, 100%) and 139/140 ($[Ni(gly)_2(H_2O)_2](H_2O)_2^{2+}$, 45%). The relative intensity of the peaks m/z 75/76 (1:1 complex, $[Ni(gly)(H_2O)]^{2+}$) is smaller (38%). Complexes containing ala or ser also produce mainly ions containing two equivalents of amino acids (main peaks m/z 135/136 ($[Ni(ala)_2(H_2O)_2]^{2+}$) and 142/143 ($[Ni(ser)_2(H_2O)]^{2+}$), respectively).

Table 5
XRD lines positions and relative intensities for nickel bisglycinate and the phase prepared from HC

$[Ni(gly)_2(H_2O)_2]$			$[Ni(gly)_2(H_2O)_2]$ (HC)		
2Θ (deg)	d (Å)	I/I_{max}	2Θ (deg)	d (Å)	I/I_{max}
13.04	6.789	100	12.26	7.219	100
16.94	5.234	84	15.76	5.623	17
18.38	4.827	12	19.04	4.661	9
18.80	4.720[a]	94	19.84	4.475	24
20.62	4.307	13	21.18	4.195	2
23.20	3.834	10	22.54	3.945	1
24.10	3.693	47	23.52	3.782	17
24.68	3.607	21	24.54	3.627	4
25.08	3.551	15	26.22	3.399	1
26.18	3.404	1	27.04	3.297	8
27.10	3.290[a]	40	28.34	3.149	5
29.02	3.077[b]	19	28.76	3.104	1
29.52	3.026	2	29.12	3.066	6
29.86	2.992	1	29.30	3.048	1

[a]Includes two diffraction lines (Supplementary material, Table S1).
[b]Includes three diffraction lines (Supplementary material, Table S1).

In contrast, for the unknown phase $[Ni(gly)_2(H_2O)_2]$ (HC), the peak corresponding to monoglycinate ion $[Ni(gly)(H_2O)]^{2+}$ reaches a relative intensity of 100%, on a par with bisglycinate species $[Ni(gly)_2(H_2O)_2](H_2O)_2^{2+}$ and $[Ni(gly)_2(H_2O)_2](H_2O)_4^{2+}$. Actually, several species containing only one equivalent of glycine are detected, such as m/z 84/85 ($[Ni(gly)(H_2O)_2]^{2+}$), 93/94 ($[Ni(gly)(H_2O)_3]^{2+}$) and 102/103 ($[Ni(gly)(H_2O)_4]^{2+}$), all around 40% of relative intensity. It can be concluded that (i) $[Ni(gly)_2(H_2O)_2]$ (HC) contains monoglycinate species or species that form monoglycinate complexes upon contact with water, and (ii) for an identical stoichiometry, the bonding between water, glycine and Ni(II) differs from that encountered in crystallized $[Ni(gly)_2(H_2O)_2]$.

The differences between $[Ni(gly)_2(H_2O)_2]$ and $[Ni(gly)_2(H_2O)_2]$ (HC) are evidenced by IR (Fig. 6, which compares these two compounds with an *in situ* spectrum recorded for $[Ni(gly)_2(H_2O)_2]$ after dehydration at 150 °C). Interpretation of the spectra is based on Refs. [27–29,36], but the attribution of some bands in the middle IR region is not straightforward because of vibrations couplings. In case of conflicting analyses, assignment based on isotope-labelled molecules has been favoured [29].

Beside some shifts in the ν_{NH} (3275–3360 cm^{-1}) and ν_{CH} (2940–3000 cm^{-1}) regions, the spectra of $[Ni(gly)_2(H_2O)_2]$

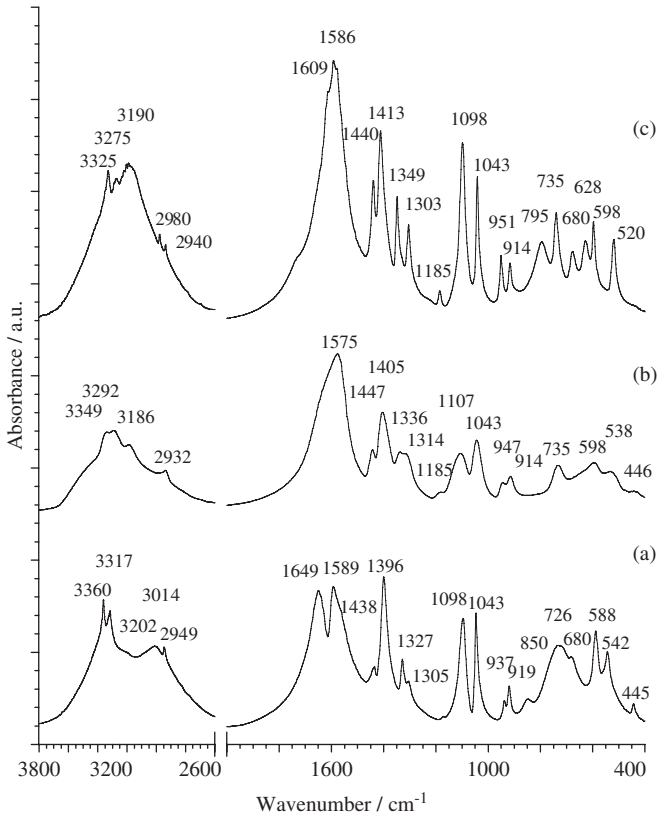

Fig. 6. Infrared spectra recorded at room temperature of (a) $[Ni(gly)_2(H_2O)_2]$ (HC), (b) dehydrated $[Ni(gly)_2(H_2O)_2]$ and (c) $[Ni(gly)_2(H_2O)_2]$. Spectra (a) and (c) have been recorded in transmission in KBr, spectrum (b) in diffuse reflectance mode.

(HC) and $[Ni(gly)_2(H_2O)_2]$ differ on three points:

- The decrease or disappearance of the bands associated to H_2O, as in the case of dehydrated $[Ni(gly)_2(H_2O)_2]$: 3190 (ν(OH)), 795 ($\rho(OH_2)$), 628 cm^{-1} (δ(OH)).
- Shifts or new bands corresponding to the CH_2-COO^- moiety: 1396 cm^{-1} for $\nu_s(COO^-)$, 1327 cm^{-1} for $\omega(CH_2)$ (supplementary band observed by Raman), 937 cm^{-1} for ν(CC), 542 cm^{-1} for ν(COO), (supplementary band also observed by Raman). However, the shift of $\nu_{as}(COO^-)$ at 1589 cm^{-1} is minor.
- Most bands corresponding to the C-NH_2 moiety are not significantly shifted (1305 cm^{-1} (tw(NH_2)), 1098 cm^{-1} ($\omega(NH_2)$), 1043 cm^{-1} (ν(N)), except the strong band at 1649 cm^{-1} which can be interpreted as $\delta(NH_2)$ shifted from 1609 cm^{-1}. It should be noted though that the ν_{as}(COO) vibration of free COOH groups has been reported at that position in Ni(II) complexes containing aspartic acid [37].

Finally, no band due to NH_3^+ is seen, suggesting the absence of zwitterionic gly, totally or partly dissociated from Ni(II), as in $[(NH_3^+CH_2COO^-)Ni(H_2O)_5]^{2+}$ for instance [38].

On the basis of those results and hypotheses on the structure of dehydrated $[Ni(gly)_2(H_2O)_2]$ in which COO^- groups are bonded to two Ni(II) cations [39], it can be proposed that in $[Ni(gly)_2(H_2O)_2]$ (HC), some glycinates have dissociated from Ni(II) by their NH_2 end, or may act as ligands bridging two Ni(II) *via* their COO^- end. Some water formerly coordinated to Ni(II) could be released in crystallization position and the band at 1649 cm^{-1} could include a contribution from the water bending mode [27].

4. Discussion

By varying the type of synthesis and Ni(II) precursor, a series of $Ni(OH)_2$ samples was prepared with different crystalline type, crystallinity and degree of organization at the atomic and microscopic levels. The results obtained are consistent with literature data. Authors report the presence of anions retained up to a high content for both α and β nickel hydroxide [18,20] and they link the small particles size and poor crystallinity of platelets to a higher amount of adsorbed water [20], the presence of distortions and microstrains along the *c*-axis [40] and a decomposition occurring at lower temperatures [40].

The morphology of hydroxide H (Aldrich) is similar to that of samples prepared by spraying [41]. This could explain why it is different from morphologies of the other β hydroxides prepared by precipitation, which, along with HT, exhibit hydroxide particles of small size in different amounts. Whether the hydroxide is of type α or β, this work suggests that the particles small size and disorganization strongly favour the fast dissolution of the hydroxide upon contact with amino acids. Cl^- ions, coming from Ni(II) chloride, favour both the poor organization of the phase and formation of smaller particles. In line with Hui et al. [42], we have assumed that Cl^- ions remain bonded to Ni(II) in the hydroxide, possibly substituting OH^- ions in the sheets. Actually, Cl^- ions are bonded to Ni(II) in solid nickel chloride [43] and even in concentrated solutions of $NiCl_2$, the proportion of Cl^- bonded to Ni(II) is high (10–50% of nickel in solution [26]). This bonding could last during hydroxide precipitation. Being larger than hydroxides, Cl^- ions (1.67 Å compared with 1.23 Å [44]) would contribute to the distortions evidenced by XRD.

The bidentate coordination of glycinates to HChl particles could suggest that the most reactive sites are located at particles edges and not on more organized basal planes with less accessible Ni(II), in line with the smaller reactivity of well-crystallized H. This is also in line with conclusions of Deabate et al. [22]; smaller crystallites are associated to a greater extent of species adsorbed on crystallites edges, which causes perturbations in the crystal lattice. It could be extrapolated that Cl^- ions present at the periphery of particles prevent their growth during formation of the hydroxide. In the pH range 6–7, the hydroxide is barely charged and no electrostatic interaction is expected with zwitterionic $NH_3^+CH_2COO^-$, predominant in solution [11]. Once the COO^- end has reacted with Ni(II) accessible sites, the closure of the chelation ring around Ni(II) is accompanied by the release of a proton from NH_3^+, which probably contributes to break the chemical bonds between Ni(II) and the hydroxide surface.

It can be noted that it was not possible to reach a yield higher than 60% following the procedure of complexes synthesis described, for two reasons. First, one can suppose that the proportion of 1:1 complexes in solution is not negligible, as shown with histidine [1]. Second, attempts to concentrate the solutions containing nickel bisglycinate resulted in the formation of an unwanted phase, related to $[Ni(gly)_2(H_2O)_2]$ but in which the bonding of the ligands is different. It is supposed that $[Ni(gly)_2(H_2O)_2]$ (HC) contains polymeric entities, in which glycinate ligands are less strongly bonded to Ni(II) than in the bisglycinate chelate. Such perturbations in Ni(II) coordination sphere would appear when water is in deficit during synthesis but may also be triggered by small quantities of nitrate or carbonate ions coming from the solid precursor and which may act as ligands to nickel ions. This confirms the importance of the choice of the salt used for the hydroxide precipitation since this phase, whose properties in solution differ from those of nickel bisglycinate, was not distinguished from the latter on the basis of chemical analyses only.

5. Conclusions

The synthesis of neutral bis(aminocarboxylato)–Ni(II) complexes involves the reaction of a solid precursor, here $Ni(OH)_2$, with an amino acid in solution. The rate of dissolution—thus of formation of the complex—is found to be related to the physicochemical characteristics of the solid, which themselves depend on the salt used to prepare the hydroxide and on the impurities the hydroxide

contains. The highest rate of dissolution is attained with particles of $Ni(OH)_2$ prepared from nickel chloride which are small, disorganized (possibly because of the presence of chloride impurities remaining bonded to nickel cations) and rich on edges sites, supposed to be the most reactive sites during hydroxide dissolution promoted by the amino acid. The choice of this hydroxide also allows one to avoid crystallization of an unwanted phase of the same composition as $[Ni(gly)_2(H_2O)_2]$, maybe polymeric, whose behaviour in solution differs from that of bis glycinate chelate. The formation of this other form of nickel glycinate may be related to the presence of nitrate or carbonate impurities in the solid precursor which perturb the complex crystallization.

Acknowledgments

The authors would like to thank Dr. Jean-Marc Krafft and Anne-Marie Blanchenet (Laboratoire de Réactivité de Surface, Université Pierre et Marie Curie) for their help in carrying out Raman and SEM experiments, respectively. Dr. Thibaud Coradin and Patrick Le Griel (Laboratoire de Chimie de la Matière Condensée, Université Pierre et Marie Curie) are also warmly thanked for providing access to the SEM microscope and for their assistance during the experiments. Sophie Rochut is thanked for carrying out MS electrospray experiments. Vicente Rodríguez-González acknowledges the Consejo Nacional de Ciencia y Tecnología (Conacyt) from Mexico for providing a grant.

Appendix A. Supplementary materials

Supplementary data associated with this article can be found in the online version at doi:10.1016/j.jssc.2007.10.015.

References

[1] L.E. Valenti, C.P. De Pauli, C.E. Giacomelli, J. Inorg. Biochem. 100 (2006) 192.
[2] (a) O. Pineda, H.D. Ashmead, Nutrition 17 (2001) 381;
(b) E. Hertrampf, M. Olivares, Int. J. Vitam. Nutr. Res. 74 (2004) 435.
[3] V. Rodríguez-González, E. Marceau, P. Beaunier, M. Che, C. Train, J. Solid State Chem. 180 (2007) 21.
[4] A.J. Stosick, J. Am. Chem. Soc. 67 (1945) 365.
[5] D.N. Sen, S. Mizushima, C. Curran, J.V. Quagliano, J. Am. Chem. Soc. 77 (1955) 211.
[6] K.A. Fraser, M.M. Harding, J. Chem. Soc. A (1967) 415.
[7] J.A. Muir, A. Ortiz, J. Appl. Crystallogr. 10 (1977) 489.
[8] T. Sakurai, H. Iwasaki, T. Katano, Y. Nakahashi, Acta Crystallogr. B 34 (1978) 660.
[9] S.R. Ebner, B.J. Helland, R.A. Jacobson, R.J. Angelici, Inorg. Chem. 19 (1980) 175.
[10] E.E. Castellano, O.R. Nascimento, R. Calvo, Acta Crystallogr. B 38 (1982) 1303.
[11] C. Ludwig, J.L. Devidal, W.H. Casey, Geochim. Cosmochim. Acta 60 (1996) 213.
[12] X. Carrier, J.F. Lambert, M. Che, J. Am. Chem. Soc. 119 (1997) 10137.
[13] X. Carrier, J.B. d'Espinose de la Caillerie, J.F. Lambert, M. Che, J. Am. Chem. Soc. 121 (1999) 3377.
[14] P. Burattin, M. Che, C. Louis, J. Phys. Chem. B 101 (1997) 7060.
[15] K. Bourikas, J. Vakros, C. Cordulis, A. Lycourghiotis, J. Phys. Chem. B 107 (2003) 9441.
[16] P.H. Tewari, A.B. Campbell, J. Colloid Interf. Sci. 55 (1976) 531.
[17] S. Le Bihan, M. Figlarz, J. Cryst. Growth 13/14 (1972) 458.
[18] P.V. Kamath, G.H.A. Therese, J. Gopalakrishan, J. Solid State Chem. 128 (1997) 38.
[19] M. Akinc, N. Jongen, J. Lemaître, H. Hofmann, J. Eur. Ceram. Soc. 18 (1998) 1559.
[20] A. Delahaye-Vidal, B. Beaudoin, N. Sac-Epée, K. Tekaia-Elhsissen, A. Audemer, M. Figlarz, Solid State Ionics 84 (1996) 239.
[21] M. Rajamathi, G.N. Subbanna, P.V. Kamath, J. Mater. Chem. 7 (1997) 2293.
[22] S. Deabate, F. Fourgeot, F. Henn, J. Power Sources 87 (2000) 125.
[23] M. Taibi, S. Ammar, N. Jouini, F. Fiévet, P. Molinié, M. Drillon, J. Mater. Chem. 12 (2002) 3238.
[24] P. Oliva, J. Leonardi, J.F. Laurent, C. Delmas, J.J. Braconnier, M. Figlarz, F. Fiévet, A. de Guibert, J. Power Sources 8 (1982) 229.
[25] M. Rajamathi, P.V. Kamath, J. Power Sources 70 (1998) 118.
[26] J. Ji, W.C. Cooper, Electrochim. Acta 41 (1996) 1549.
[27] M. Meng, L. Stievano, J.F. Lambert, Langmuir 20 (2004) 914.
[28] M.T. Rosado, M.L.T.S. Duarte, R. Fausto, Vib. Spectrosc. 16 (1998) 35.
[29] G.C. Percy, H.S. Stenton, J. Chem. Soc. Dalton Trans. (1976) 1466.
[30] S.G. Teoh, B.T. Chan, H.K. Fun, M.E. Kamwaya, Z. Kristallogr. 181 (1987) 199.
[31] D. van der Helm, M.B. Hossain, Acta Crystallogr. B 25 (1969) 457.
[32] J. Li, C. Ge, J. Fang, Cryst. Res. Technol. 25 (1990) K93.
[33] J. Li, C. Ge, G. Pan, Cryst. Res. Technol. 25 (1990) K99.
[34] J. Li, C. Ge, Y. Zhang, Cryst. Res. Technol. 25 (1990) K5.
[35] F. Négrier, E. Marceau, M. Che, J.M. Giraudon, L. Gengembre, A. Löfberg, J. Phys. Chem. B 109 (2005) 2836.
[36] J.R. Kincaid, K. Nakamoto, Spectrochim. Acta A 32 (1976) 277.
[37] O. Versiani Cabral, C.A. Téllez S., T. Giannerini, J. Felcman, Spectrochim. Acta A 61 (2005) 337.
[38] J. Peterková, J. Podlahová, J. Loub, Z. Mička, Acta Crystallogr. C 47 (1991) 2664.
[39] C.A. McAuliffe, W.D. Perry, J. Chem. Soc. A (1969) 634.
[40] J.M. Fernández Rodríguez, J. Morales, J.L. Tirado, J. Mater. Sci. 21 (1986) 3668.
[41] J. Chen, D.H. Bradhurst, S.X. Dou, H.K. Liu, J. Electrochem. Soc. 146 (1999) 3606.
[42] L. Hui, D. Yunchang, Y. Jionglang, W. Zeyun, J. Power Sources 57 (1995) 137.
[43] J. Mizuno, J. Phys. Soc. Jpn. 16 (1961) 1574.
[44] R.D. Shannon, Acta Crystallogr. A 32 (1976) 751.